ELSEVIER

Journal of Power Sources 100 (2001) 29–46

JOURNAL OF POWER SOURCES

www.elsevier.com/locate/jpowsour

Valve-regulated lead-acid batteries

D. Berndt*

Formerly VARTA Batterie AG, Am Weissen Berg 3, 611476 Kronberg, Germany

Abstract

Valve-regulated lead-acid (VRLA) batteries with gelled electrolyte appeared as a niche market during the 1950s. During the 1970s, when glass-fiber felts became available as a further method to immobilize the electrolyte, the market for VRLA batteries expanded rapidly. The immobilized electrolyte offers a number of obvious advantages including the internal oxygen cycle which accommodates the overcharging current without chemical change within the cell. It also suppresses acid stratification and thus opens new fields of application. VRLA batteries, however, cannot be made completely sealed, but require a valve for gas escape, since hydrogen evolution and grid corrosion are unavoidable secondary reactions. These reactions result in water loss, and also must be balanced in order to ensure proper charging of both electrodes. Both secondary reactions have significant activation energies, and can reduce the service life of VRLA batteries, operated at elevated temperature. This effect can be aggravated by the comparatively high heat generation caused by the internal oxygen cycle during overcharging. Temperature control of VRLA batteries, therefore, is important in many applications.

Keywords: Lead-acid battery; VRLA battery; Acid stratification; Grid corrosion; Self-discharge; Heating effects in batteries

1. Introduction

Lead-acid batteries represent the oldest rechargeable battery system and despite their rather limited storage capability, they have maintained their leading position in the market for more than 100 years. Besides their moderate price, a number of attributes favor the use of lead-acid batteries. One of these is their suitability for standby applications, which is exploited in many stationary applications and also in the vast field of motor cars where the ''starter battery'' not only starts the engine but also supplies energy in standstill periods and stabilizes the voltage of the electrical network in the car.

The valve-regulated version of this battery system, the VRLA battery, is a development parallel to the sealed nickel/cadmium battery that appeared on the market shortly after World War II and largely replaced lead-acid batteries in portable applications at that time. These batteries are characterized by immobilized electrolyte that allows an internal oxygen cycle which absorbs overcharging current, so that oxygen does not escape from the cell. The lead-acid battery, however, cannot be made totally sealed, but has to have a valve for the escape of small portions of gas, even under normal operational conditions, since hydrogen evolution is always present as a slow, but unavoidable secondary reaction.

1.1. History

The internal oxygen cycle requires open space within the cell that allows fast diffusion of oxygen in the gaseous phase. In sealed nickel/cadmium batteries this is achieved by absorption of the electrolyte by a fiber felt where larger pores remain empty. This method initially could not be copied for the lead-acid chemistry, since the plastic fibers then available were not sufficiently wetted by acid and the felt soon became filled by gas bubbles that hindered current flow. An alternative method to immobilize the electrolyte proved to be suitable, however, namely the formation of a gel by adding silicon dioxide to the sulfuric acid electrolyte. Such an ''immobilization'' was known from the manufacture of primary batteries where wheat flour (mainly) is used as a thickener of the electrolyte in the so-called ''dry batteries''. In lead-acid batteries, the formation of gelled electrolyte initially was also aimed to prevent spilling of the acid on portable applications. But soon it became evident, that in such a gelled electrolyte, space for fast oxygen transport is also left in cracks. Based on this method, SONNENSCHEIN dryfit batteries were the first VRLA batteries, manufactured on a large scale since the 1950s. An example is shown in Fig. 1.

* Tel.: +49-6173-32-2680; fax: +49-6173-32-2680.
E-mail address: dr.d.berndt@netart-net.de (D. Berndt).

0378-7753/01/$ – see front matter
PII: S0378-7753(01)00881-3

Fig. 1. VRLA batteries manufactured in the 1950s by SONNENSCHEIN (Fig. 3.1 in [1]).

These batteries had mainly been developed as a less expensive substitute for sealed nickel/cadmium batteries in photo-flashlights, tape recorders and similar portable applications, but also gradually became introduced into stationary applications, like small alarm displays and emergency lights. During the first years, they were only manufactured in small sizes up to about 10 Ah.

An important change occurred in the 1970s, when micron diameter glass fibers, which originally had been developed for air filters, appeared in the market. These are excellently wetted by sulfuric acid and, furthermore, they prevent the penetration of lead dendrites that might be formed at the negative electrode. Hence, such glass mats can absorb the electrolyte and simultaneously act as separator. The first battery that used this technique was the ''CYCLON'' manufactured by GATES. It is shown in Fig. 2.

The spiral battery design, which is still on the market (cf. Fig. 18), employs one positive and one negative

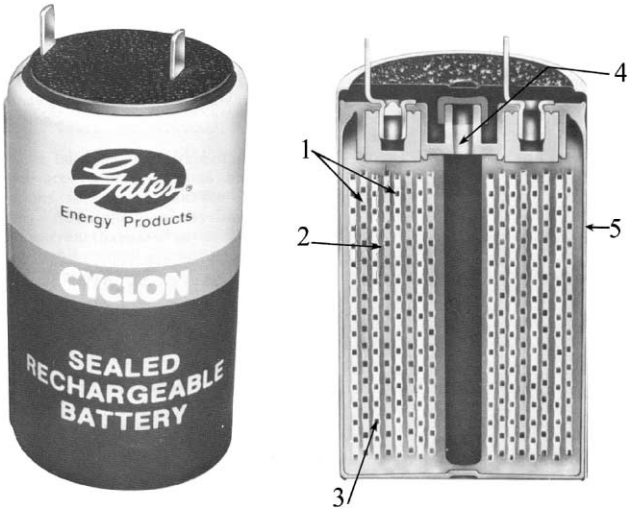

Fig. 2. Cyclon cell cross section on the right: (1) positive and negative plates; (2) separator (AGM: absorbing glass mat); (3) pure lead grids; (4) safety vent; (5) metal enclosure. Originally offered as 2.5, 5, 12.5 and 25 Ah cells; GATES [2], now HAWKER.

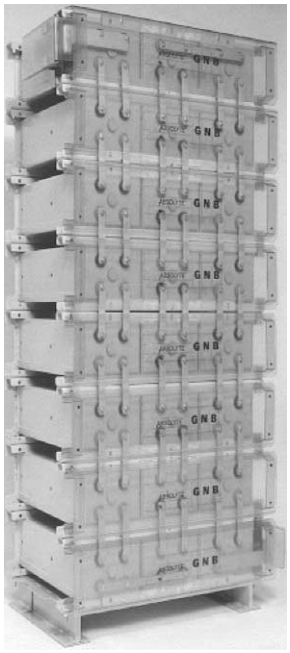

Fig. 3. Large 48 V stationary battery cells with AGM separator GNB Absolyte [3].

electrode which are wound together with the separator between them.

The absorbent glass mat (AGM) separator strongly stimulated further development and this was supported by the move to decentralize the emergency-energy supply in telephone networks leading to the requirement to place the batteries close to the electric equipment. Soon larger prismatic cells also appeared on the market for stationary applications, and nowadays VRLA batteries based on both, AGM and gelled electrolyte, are available in the capacity range between 1 and 3000 Ah for both stationary and motive power applications. Fig. 3 shows a large stationary battery with horizontally positioned cells.

Fig. 3 clearly shows an advantage that emerges from the possibility to operate VRLA batteries either in a vertical or in a horizontal position; the foot print of a large battery can be kept rather small, provided that the bearing capacity of the floor is high enough. Such an arrangement simultaneously provides easy access to the terminals of each cell for measuring purposes.

2. The electrochemical system of the lead-acid battery

The lead-acid battery represents a rather complex electrochemical system of primary and secondary reactions. The discharging–charging reactions are based on the conversion of lead (Pb) and lead dioxide (PbO_2) into lead sulfate ($PbSO_4$) and its reversal according to:

Positive electrode :

$$PbO_2 + H_2SO_4 + 2H^+ + 2e^- \Leftrightarrow PbSO_4 + 2H_2O \quad (1a)$$

Negative electrode :

$$Pb + H_2SO_4 \Leftrightarrow PbSO_4 + 2H^+ + 2e^- \quad (1b)$$

Cell reaction :

$$Pb + PbO_2 + 2H_2SO_4 \Leftrightarrow 2PbSO_4 + 2H_2O \quad (1)$$

The nominal equilibrium voltage amounts to $E_0 = 2.0$ V, given by the difference between the equilibrium values of the electrode reactions $E_{0,PbSO_4/PbO_2} = 1.7$ V and $E_{0,Pb/PbSO_4} = -0.3$ V (which to some extent depends on acid concentration (cf. e.g. [4], p. 103).

There are, however, secondary reactions that occur at electrode potentials within the cell voltage, e.g. water decomposition according to:

Oxygen evolution at the positive electrode :

$$2H_2O \Rightarrow O_2 + 4H^+ + 4e^- \quad (2a)$$

Hydrogen evolution at the negative electrode :

$$4H^+ + 4e^- \Rightarrow 2H_2 \quad (2b)$$

Overall water decomposition :

$$2H_2O \Rightarrow O_2 + 2H_2 \quad (2)$$

The equilibrium voltage of this reaction is $E_0 = 1.23$ V (given by the difference $E_{0,H_2O/O_2} = 1.23$ V; minus $E_{0,H^+/H_2} = 0$ V), and is much smaller than the nominal voltage of the lead-acid battery.

Furthermore, at an electrode potential below 1.23 V, the reversal of Eq. (2a) is possible, according to:

$$O_2 + 4H^+ + 4e^- \Rightarrow 2H_2O \quad (3)$$

which means that reduction of oxygen always is to be expected at the negative electrode.

As a further problem, at the high potential of the positive electrode all metals are destroyed by oxidation. This includes lead which in principle, starts to corrode at the potential of the negative electrode according to the discharge reaction $Pb \Rightarrow PbSO_4$. At the potential of the positive electrode, lead is further oxidized to PbO_2 which forms a protecting layer according to:

$$Pb + 2H_2O \Rightarrow PbO_2 + 4H^+ + 4e^- \quad (4)$$

However, this layer is not quite stable, and some corrosion continues (cf. Section 4.1.2).

As a consequence, the following unwanted reactions are always present in a lead-acid battery:

1. oxygen evolution at the positive electrode;
2. oxygen reduction at the negative electrode;
3. hydrogen evolution at the negative electrode and
4. grid corrosion.

Fig. 4 illustrates the situation. The horizontal axis shows the potential scale referred to the standard hydrogen electrode; the range of the negative electrode on the left hand, the range of the positive electrode on the right hand. In the center, a range of about 1.2 V is omitted in order to stretch the scale. The rates of the various reactions are represented by *current–voltage curves* that indicate how the rate of the reaction in question, expressed as current equivalent, depends on polarization.

The two hatched columns represent the equilibrium potentials of the negative and positive electrodes, respectively. Their dependence on acid concentration is indicated by the width of these columns. The *charging* and *discharging* reactions are represented by the broken curves. They are very steep, since these reactions are fast, and occur at a high rate even at a small deviation from the equilibrium potential.

Fig. 4 shows that hydrogen and oxygen evolution already occur at the open-circuit potential of the negative and positive electrodes, respectively. The gradual initial increase of the corresponding curves indicates that these reactions occur slowly, as long as the potential difference relative to

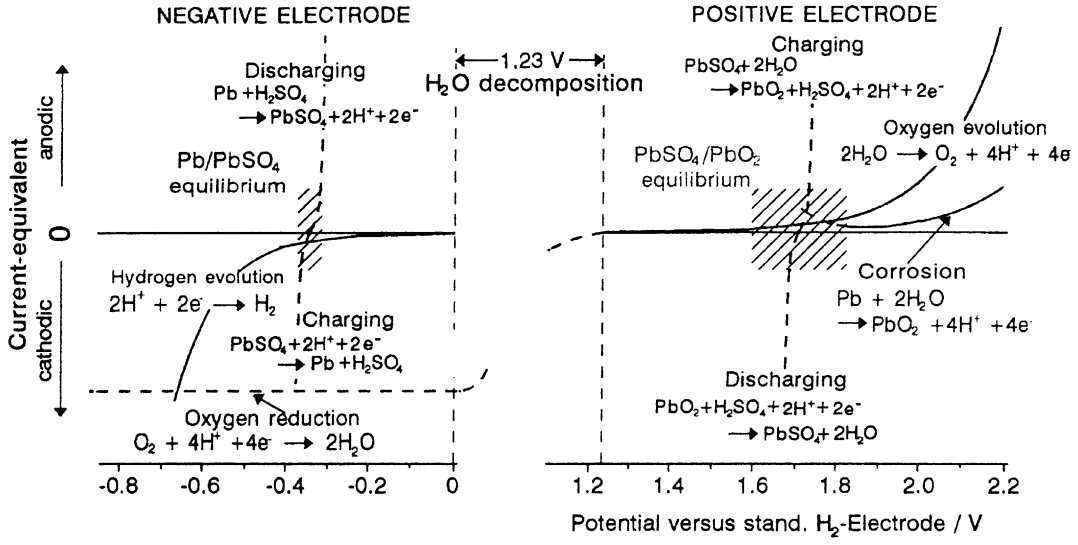

Fig. 4. Reactions that occur in lead-acid batteries plotted vs. electrode potential. The rates of these reactions are indicated by current potential curves.

their origin, the ''polarization'' or ''overvoltage'', remains fairly small. When, however, this deviation from the equilibrium potential exceeds a certain value, the two curves show a steep increase. This means that hydrogen as well as oxygen generation gain in volume enormously at low and high overvoltage, respectively.

Fig. 4 indicates a slight minimum of the corrosion reaction at about 40–80 mV above the $PbSO_4/PbO_2$ potential. At an electrode potential below this minimum, corrosion increases due to destabilization of the protecting layer. Above this minimum, the corrosion rate follows the usual exponential increase with increasing electrode potential.

The rate of oxygen reduction (according to Eq. (3)) is largely determined by the rate of oxygen transport and, therefore, does not depend on the potential of the negative electrode. It is characterized as a ''limiting current'' by the horizontal curve in Fig. 4. In conventional batteries with liquid electrolyte, this limiting current is very small, since the diffusion rate of dissolved oxygen is very slow, and as consequence, the equivalent of oxygen reduction is limited to a few mA per 100 Ah of nominal capacity and thus is hardly noticed in battery practice.

3. The valve-regulated version

The VRLA battery is based on the same materials and electrode reactions as the conventional version. The main difference is the immobilization of the electrolyte and the internal oxygen cycle thereby achieved. Immobilization means that the electrolyte is soaked into an adsorbent glass mat or is gelled by addition of SiO_2. In both cases, no liquid electrolyte is left within the cell which consequently can be operated in different positions as is shown in Fig. 3. Further, the immobilized electrolyte hinders or eliminates stratification of the acid and opens new applications for lead-acid batteries as described in the next section.

In the immobilized electrolyte, open space is left in the larger pores of the AGM felt which are not filled by electrolyte or in cracks in the gelled electrolyte and this allows fast oxygen transport by diffusion in the gaseous phase, which is more than 10^5 times faster than in the dissolved state. Gas phase diffusion of oxygen is even fast enough to by-pass the separator that is required with a gelled electrolyte. As a consequence, oxygen has to pass in the dissolved state only a thin wetting layer at the surface of the negative electrode. Thus, oxygen reduction according to Eq. (3) becomes a very fast reaction, and oxygen which is generated at the positive electrode, does not leave the cell but is reduced at the negative electrode and forms the internal oxygen cycle.

3.1. Acid stratification

The immobilization of the electrolyte has a side effect of enormous practical importance: it eliminates stratification of the electrolyte, at least to a large extent. This stratification is caused by the peculiar situation of the lead-acid battery that the sulfuric acid in the electrolyte participates in the electrode reaction, as is obvious in Eq. (1). The stratification of the electrolyte which results is illustrated in Fig. 5.

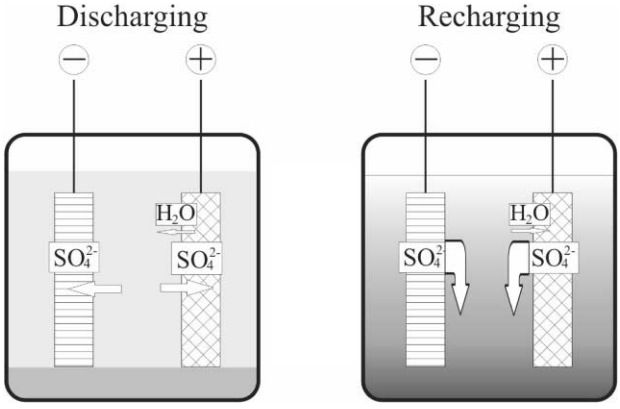

Fig. 5. The development of acid stratification in lead-acid batteries with liquid electrolyte.

When the battery is discharged, the concentration of the acid is reduced, since SO_4^{2-} ions are absorbed by both electrodes according to Eqs. (1a) and (1b), and in addition, water is generated at the positive electrode according to Eq. (1a), as indicated in the left-hand part of Fig. 5. Acid consumption occurs in the pores of the active material, and thus reduces the specific gravity of the electrolyte close to the electrode surface. This causes an upward flow which mixes the bulk of the electrolyte between, and above, the electrodes. At the end of discharge, the concentration of the acid is lower, but more or less uniform, apart from that which is localized below the electrodes and which had not been included in the flow pattern due to its higher density. Complete uniformity of all the acid would only be reached by diffusion after a prolonged period of time.

When the battery is recharged, SO_4^{2-} ions are released from the electrodes and water is consumed by the positive electrode. Thus, the acid concentration in a layer close to the surface of the electrodes is increased, especially at the positive electrode, and its higher specific density initiates a downward movement. Thus, the acid at the bottom becomes increasingly concentrated, and when such partly discharging–charging cycles are repeated without acid mixing, the acid at the top becomes progressively diluted, while at the bottom, the concentration may exceed the original value significantly, as indicated in the right-hand part of Fig. 5. The consequence of such a stratification is that, in the upper part of the electrodes, the active material is only partly utilized due to lack of acid, while in the bottom zone of both electrodes, it is overstressed. Thus, in the bottom part disintegration of the active material in the positive electrode and sulfation in the negative electrode are the results that will cause premature failure of the battery.

For this reason, vented lead-acid batteries with liquid electrolyte are not suited for such partly discharging–char-

ging schedules, rather they have regularly to be overcharged (a total recharge of about 115% may be required) to eliminate acid stratification. During such overcharging periods, the heavy gassing produces bubbles that ascend within the electrolyte and so cause mixing. More effective mixing is achieved by forced acid agitation with the aid of inserted air-lift pumps. For such batteries, an overcharge factor of 104% is sufficient (cf. e.g. [4], p. 258).

In VRLA batteries, the immobilized electrolyte greatly hinders the vertical flow of the acid. The more effectively is the acid immobilized, the less stratification occurs. (This is one reason to use very fine fibers that form correspondingly fine pore systems with high capillary forces for AGM separators [5].) As a consequence, only very small stratification effects are observed in AGM felts, and the strong bond of the acid in the gelled electrolyte is the reason why such batteries do not show any stratification effects. The reduction or elimination of stratification allows the use of VRLA batteries in applications where acid mixing cannot be achieved by overcharging, and where conventional lead-acid batteries suffer premature failure due to acid stratification. Such applications include automatic guided transport vehicles where only intermediate boost charges that do not fully recharge the battery are possible. Batteries in taxi cars also show a significantly improved service life in the VRLA version, since their duty cycle does not always allows them to be fully charged. In stationary applications, VRLA batteries perform better than flooded batteries as standby storage for wind and solar energy generation. These batteries cannot be recharged regularly and properly, since the required energy is not always available. Recently, VRLA batteries with AGM separators have also been reported to operate properly in "peak shaving" applications where the battery is continuously partly discharged and recharged at an average state of charge of about 80% [6].

4. Secondary reactions in VRLA batteries

When the battery is overcharged, in principle, the same secondary reactions occur in the vented and the VRLA system, but their weighting is quite different.

- In the vented version, with liquid electrolyte, oxygen and hydrogen evolution are the main secondary reactions. Both gases escape from the battery and cause water loss that approximately corresponds to the overcharging current. Oxygen reduction and corrosion are comparatively small and hardly noticed as competing reactions.
- In the VRLA battery, oxygen which is evolved at the positive electrode, is subsequently nearly completely reduced at the negative and thus remains within the cell. The main secondary reactions are oxygen evolution at the positive electrode and oxygen reduction at the negative electrode, which nullify each other. Hydrogen evolution is reduced to a low level, close to the rate of self-discharge of the negative electrode and the hydrogen evolved escapes from the cell. Water loss is correspondingly reduced, and there is no direct relation between water loss and overcharging current. The rates of hydrogen evolution and grid corrosion gain great importance, even though they are small compared to the internal oxygen cycle, since they cause water loss that cannot be compensated for, and the balance between them determines the polarization of the two electrodes.

The typical situation of a VRLA battery during overcharging is shown in Fig. 6 which is based on model calculations by Teutsch [7,8]. The horizontal axis shows the polarization of the positive and negative electrodes. On the vertical axis, the reaction rates are plotted as current equivalents on a logarithmic scale. The zero point of the horizontal axis is the open-circuit voltage of the cell, i.e. zero polarization of positive and negative electrodes.

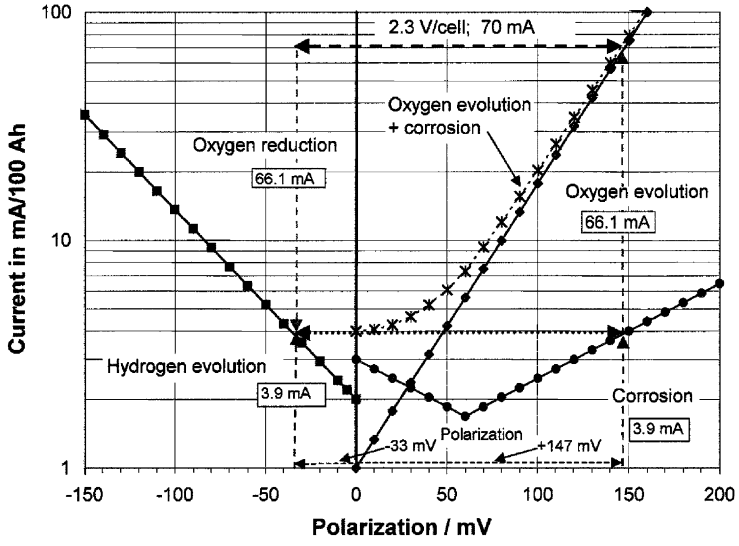

Fig. 6. Overcharging of a VRLA battery at 2.3 V per cell. The zero point of the horizontal axis (zero polarization) is assumed as $E_0 = 2.12$ V per cell which would correspond to an acid density of 1.28 g cm^{-3}. Hundred percent of recombination efficiency is assumed for the internal oxygen cycle.

In this semi-logarithmic plot, the rates of oxygen and hydrogen evolution are represented by TAFEL lines. The figure shows the typical slopes per decade of current increase of −120 and +80 mV for hydrogen and oxygen generation, respectively. In this example at open circuit, i.e. zero polarization, oxygen and hydrogen evolution correspond to 1 and 2 mA/100 Ah, respectively. The latter would be equivalent to a self-discharge of the negative of 1.44 Ah per month or 1.44% per month. Such data are of course influenced by the specific parameters of the cell concerned.

The corrosion behavior is approximated by the combination of two TAFEL lines. This corresponds to practical experience and describes the minimum of corrosion at 40–80 mV above the open-circuit potential of the positive electrode that is indicated in Fig. 4. The slope of this TAFEL line is 240 mV per decade which is in accordance with general experience, and indicates that corrosion increase with potential is smaller than that of oxygen evolution.

Hundred percent of recombination efficiency is assumed in Fig. 6 which means that all the oxygen that is evolved at the positive electrode subsequently is reduced at the negative. In practice, the efficiency comes close to this value and usually reaches at least 98%. (Actually, 100% of recombination efficiency can only be approximated, since a certain partial pressure of oxygen always exists within the cell and a corresponding portion of oxygen is lost together with the escaping hydrogen.)

Polarization of the electrodes and the resulting current equivalents are determined by the primary rule: ''the same current must flow through both electrodes as soon as the charging or discharging current circuit is closed''.

This means that the current equivalents of hydrogen evolution and oxygen reduction at the negative electrode together must equal the sum of oxygen evolution and grid corrosion at the positive electrode. Otherwise, the current circuit would not be closed. This condition is only fulfilled at one particular value of the polarization of the two electrodes, which occurs automatically. (There is only one possibility to fulfill this rule as indicated in Fig. 6 by the horizontal double arrow that marks the current of 70 mA.) In this example, it means that the positive and the negative electrodes are polarized to 147 and −33 mV, respectively. The 147 mV of polarization cause an oxygen evolution rate of 66.1 mA/100 Ah, and a corrosion of 3.9 mA/100 Ah, and the sum of both reactions gives the current flow through the positive electrode of 70 mA. At the negative electrode, the polarization of −33 mV results in hydrogen evolution at a rate of 3.9 mA/100 Ah which, together with the 66.1 mA/100 Ah of oxygen reduction that are determined by 100% of recombination efficiency, also amounts to 70 mA/100 Ah.

The assumption of 100% of efficiency of the internal oxygen cycle, causes the additional condition that hydrogen evolution and grid corrosion must equal each other, since both are the supplements to oxygen reduction and oxygen evolution that balance each other. This is indicated by the dotted horizontal double arrow in Fig. 6. This is a very important condition, since it means that the polarization of the electrodes in a VRLA battery is determined by the balance between hydrogen evolution and grid corrosion (cf. Section 4.2). Although this condition exactly applies only at a recombination efficiency of 100%, it more or less can generally be assumed for VRLA batteries, as has been mentioned above.

Fig. 6 indicates the typical situation of a VRLA battery during overcharging: the main reaction at the negative electrode, the reduction of oxygen needs no polarization, since its equilibrium potential of +1.23 V is far above that of the negative electrode (cf. Eq. (3)). Thus, the negative electrode must only be polarized to evolve the amount of hydrogen that compensates for the difference between current flow and oxygen evolution which is mainly given by the rate of corrosion. As a consequence, the polarization of the cell is distributed very unevenly as indicated in Fig. 6. Mainly, it is the positive electrode which is polarized, while the potential of the negative electrode remains rather close to its equilibrium value. Thus, in VRLA batteries, hydrogen evolution is reduced close to its minimum, which is the rate of self-discharge by hydrogen evolution at open circuit.

The small amount of hydrogen that is evolved has to escape from the cell. It cannot form an internal hydrogen cycle as is the case in nickel/metal hydride batteries, since hydrogen oxidation at the PbO_2 electrode is so slow that it can be neglected. The unavoidable hydrogen evolution would cause a continuous increase of the internal pressure until the cell would be destroyed. For this reason, the lead-acid battery cannot be sealed, but has to have a valve that opens from time to time and allows the escape of hydrogen, even under normal operational conditions. This gave this battery its now generally accepted name ''valve-regulated lead-acid battery'' or VRLA battery. (Sometimes the (not correct) name ''sealed lead-acid batteries'' is found in the literature, e.g. in the Federal Regulations of the USA, concerning battery disposal, they are called ''SSLA batteries (sealed small lead-acid batteries)'' cf. e.g. [9].)

4.1. Water loss

Hydrogen evolution at the negative electrode and grid corrosion at the positive electrode together cause water loss according to:

Hydrogen evolution (Eq. (2b)) :

$$4H^+ + 4e^- \Rightarrow 2H_2$$

Grid corrosion (Eq. (4)) :

$$Pb + 2H_2O \Rightarrow PbO_2 + 4H^+ + 4e^-$$

In total :

$$Pb + 2H_2O \Rightarrow PbO_2 + 2H_2 \quad (5)$$

This water loss must be kept as low as possible since it gradually increases the concentration of the electrolyte and decreases its volume, and thus influences the performance of

the battery. Water loss cannot be compensated by refilling of water. Water loss is the main reason for the slight decrease of capacity that is observed from the very beginning in cycle tests of VRLA batteries. As a consequence, the design of VRLA batteries must always have the aim to keep hydrogen evolution and grid corrosion as low as possible.

4.1.1. Hydrogen evolution

Hydrogen evolution starts about 0.3 V above the potential of the negative electrode, and thus is always present. At open circuit, it is the main self-discharge reaction of the negative electrode, provided that oxygen has no access through a defect valve or a leakage of the container. Fortunately, hydrogen evolution is extremely hindered at the lead surface and thus its rate is about 7 orders of magnitude smaller compared to hydrogen evolution rates at other metals, like nickel or copper (cf. Fig. 3 in [10]). But such an extreme hindrance of an electrochemical reaction is always precarious and can be undone by contaminants. Thus, hydrogen evolution on the lead surface would be increased enormously by the precipitation of traces of metals, like nickel and copper. A low hydrogen-evolution rate can only be achieved by the use of extremely pure lead for the active material and the alloys used as grid or conducting elements. Furthermore, all the other components of the cell must be stable, otherwise, critical substances may be leached out and contaminate the negative electrode.

The demand for highly purified materials, however, contrasts with the price, which grows considerably with increasing purity. In the near future, this question may gain in importance, since due to the growing recycling efforts of all materials, secondary lead has increasingly to be used for the active material in batteries. In the USA, nowadays 75% of the lead on the market is secondary lead and this percentage is increasing [11]. Secondary lead, may contain quite a number of additives which in their entirety determine the hydrogen-evolution rate [12], and it is a question of economics how far the various smelters can purify the lead at an acceptable price. Thus, it may become more expensive to purchase ''highly purified lead''. The consequences will be discussed in Section 4.2.2.

4.1.2. Corrosion

Above the potential of the positive electrode, the tetravalent ion (Pb^{4+}) is the stable state and this forms PbO_2. Thus, the grid material in the positive electrode is converted according to Eq. (4) into PbO_2 which forms a rather dense layer that protects the underlying lead from further corrosion. The situation at the phase boundary Pb/PbO_2, however, is not stable as indicated in Fig. 7.

The area on the left represents the grid while the active material of PbO_2 is shown on the right. Between these, a dense layer, also of PbO_2 formed by corrosion, covers the grid surface, and protects the bulk of the material. However, PbO_2 and Pb cannot exist in contact with each other for thermodynamic reasons, and a thin layer of less oxidized

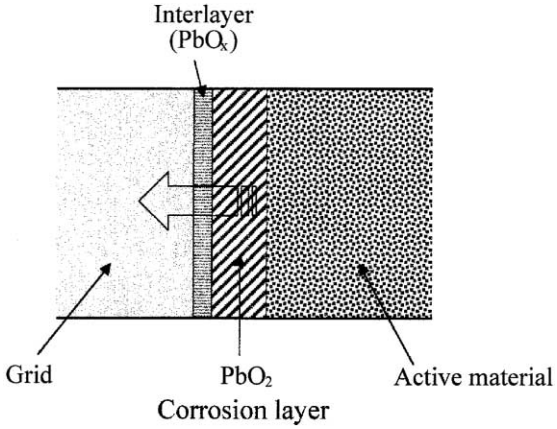

Fig. 7. Structure of the corrosion layer at the surface of the positive grid. Penetration rates between 0.005 and 0.05 mm per year are reported for alloys that are applied in VRLA batteries.

material (PbO_x) is always formed between the grid and the PbO_2. The existence of lead monoxide (PbO) in this layer has been determined; the existence of higher oxidized species is assumed, but their structure is not yet known exactly. (This intermediate layer is the main reason why periodical charges are required with lead-acid batteries during prolonged storage periods, since at open circuit, this layer gradually grows by further oxidation of the lead, while PbO_2 is reduced. Thus, the result would be

$$Pb + PbO_2 \Rightarrow 2PbO \quad (6)$$

and the protection of the grid against corrosion would be lost when the PbO layer comes into contact with the acid and forms $PbSO_4$.)

The PbO_2/PbO_x layer gradually penetrates into the grid as indicated by the arrow in Fig. 7. This process goes forward at a very slow rate mainly as a solid-state reaction. Cracks are formed when the oxide layer exceeds a given thickness, on account of the growth in volume when lead is converted into PbO_2. Underneath the cracks, the corrosion process starts again. As a result, under the usual float conditions, the corrosion proceeds at a fairly constant rate between 0.005 and 0.05 mm per year (cf. Table 2 in [10]) and never comes to a standstill. A continually flowing anodic current, the corrosion current, is required to re-established the corrosion layer.

General parameters that determine this corrosion current are

- electrode potential and
- temperature.

Two further parameters, specific to the battery concerned, are

- specific corrosion rate of the alloy employed and
- surface area of the grid.

The specific corrosion rate is a complex quantity that is not only influenced by the composition of the alloy but also by a number of further parameters, like its metallographic

structure. In general, pure lead has the lowest corrosion rate. A survey of alloys that are especially applied in VRLA batteries is given in [13].

The grid surface that is exposed to the active material and thereby to the electrolyte can vary between about 800 cm^2 in a tubular electrode and about 4000 cm^2/100 Ah of nominal capacity in a thin punched grid as is used in cylindrical cells, like the examples in Figs. 2 and 18.

Based on these values, currents between 0.3 and 10 mA/100 Ah are to be expected as corrosion currents which are required to continuously re-establish the protective layer of PbO_2 and thereby keep the situation at the grid surface stable (cf. Table 4 in [10]).

4.1.3. Temperature influence

The rate of most electrochemical reactions is approximately doubled for a temperature increase of 10°C. This applies also to hydrogen and oxygen evolution and to grid corrosion in lead-acid batteries (experimental results, e.g. [4], p. 241). Thus, the TAFEL lines are correspondingly shifted upwards with increasing temperature. (Oxygen transport by diffusion is less accelerated by temperature increase, compared to the electrochemical reactions. For this reason, a slight reduction of the recombination efficiency is to be expected with increasing temperature.)

The increase of hydrogen evolution and grid corrosion with increasing temperature has a serious effect, since according to Eq. (5), both determine the water loss of the battery. Thus, water loss may become a limiting factor of the service life. As a result, the service life of a battery that is floated continuously at the same voltage but 10°C above, the normal temperature will approximately be reduced to one-half of its normal value, while a temperature increase of 20°C will reduce the service life to one-quarter. Batteries in the field are often exposed to daily and seasonal fluctuations of temperature. Then the aging of the battery is determined by the ratio of the periods at the various temperatures [14].

For stationary batteries which are continuously overcharged (float charging), the increase of water loss and grid corrosion at elevated temperatures suggests a compensation by a corresponding reduction of the cell voltage. Such a compensation has been proposed repeatedly for vented batteries, but it has hardly been practiced. Compensation of the float voltage is mostly recommended, for VRLA batteries, but in a way that differs from manufacturer to manufacturer. The fundamental difficulty is that the float voltage cannot be reduced in a manner that completely compensates for temperature influence (cf. e.g. [4], p. 408).

4.2. Balance between hydrogen evolution and grid corrosion

Balance between hydrogen evolution and grid corrosion determines the polarization of the electrodes, as has been mentioned already in connection with Fig. 6. This is of great importance especially in stationary applications where the battery is continuously overcharged at a comparatively low voltage, since

1. the overcharging current should be as low as possible to minimize water loss and corrosion and
2. the gap between charging and discharging voltage should be as small as possible to allow uninterrupted power supply without additional switching equipment.

To emphasize the problem that may arise under such "float" conditions, in Fig. 8 the hydrogen evolution rate is

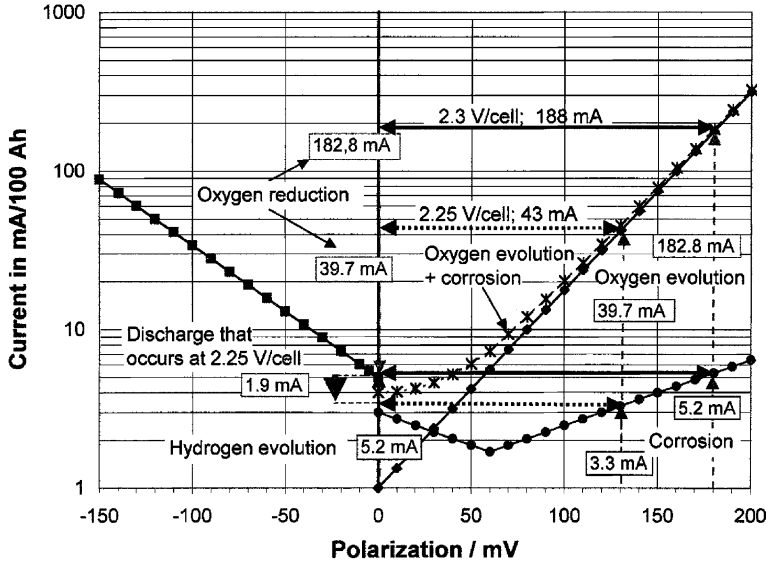

Fig. 8. Overcharging of a VRLA battery. Characteristics as in Fig. 6, except an increased hydrogen evolution by the factor 2.5. Hundred percent of recombination efficiency is assumed (zero point of polarization: $E_0 = 2.12$ V; i.e. acid density 1.28 g cm^{-3}). The dotted double arrows indicate the situation at 2.25 V per cell when hydrogen evolution at zero polarization (self-discharge) can no longer be compensated by corrosion. Then the negative electrode attains positive polarization and is gradually discharged.

assumed 2.5 times higher compared to Fig. 6, expressed by a corresponding shift of the TAFEL line in vertical direction. Thus, a clear imbalance exists between hydrogen evolution and grid corrosion. The further aggravated situation at a reduced overcharging voltage of 2.25 V per cell is also indicated.

At 2.3 V per cell, equal current flow through both electrodes is achieved only at +180 mV of polarization of the positive electrode. But then the polarization of the cell (2.3–2.12 V) is completely required for the positive electrode, while the polarization of the negative electrode is reduced to zero. The float current that is mainly determined by oxygen evolution amounts now to 188 mA/100 Ah and is composed at the positive electrode of 182.8 mA for oxygen evolution and 5.2 mA for grid corrosion and is balanced at the negative electrode by the sum of 182.8 mA for oxygen reduction and 5.2 mA for hydrogen evolution. This, however, represents a very critical situation of the negative electrode, since the slightest further increase of hydrogen evolution or a reduction of the cell voltage would cause positive polarization and this means discharge of the negative electrode.

This is clearly to be seen at the lower overcharging voltage of 2.25 V per cell which leads to a reduction of the cell polarization to 130 mV (dotted double arrows in Fig. 8). At this overcharging voltage, balance between hydrogen evolution and grid corrosion can no longer be achieved, since the self-discharge rate of the negative electrode at zero polarization exceeds grid corrosion at 130 mV of positive polarization. As a consequence, the polarization of the negative electrode is shifted to a positive value. This evokes discharge of the negative electrode as an additional (anodic) reaction that fills the gap between hydrogen evolution and grid corrosion. Only a few millivolt of positive polarization would be sufficient, since discharge is a very fast reaction. Thus, the surplus of hydrogen evolution of 5.2 mA/100 Ah is compensated by a self-discharge current equivalent to 1.9 mA/100 Ah and the resulting difference 5.2 mA − 1.9 mA = 3.3 mA balances grid corrosion.

The discharge of the negative electrode equivalent to 1.9 mA/100 Ah means a loss of capacity of 1.4 Ah per month or about 17% per year. After floating for 3 years under these conditions, the battery would have lost about 50% of its capacity, and that would not have been realized by voltage readings, since the battery is floated at the correct voltage. Even the open-circuit voltage would hardly give an indication, since its decay is much lower when only the negative electrode suffers discharge, compared to the figures often published as a possibility for a rough determination of the state of charge (cf. e.g. [15], see Fig. 9).

For this reason, it is rather difficult to detect an unbalanced cell under float conditions, except by capacity tests.

4.2.1. Oxygen intake

The balance between hydrogen evolution and grid corrosion can also be disturbed by the intake of oxygen which may be caused by a valve not properly closing or a leakage in the sealings of the container. Due to its easy access to the negative electrode, oxygen would be reduced and form an additional (anodic current) with the consequence that the electrode potential is shifted to more positive values. When the amount of oxygen exceeds the critical limit, the potential of the negative electrode will be shifted to positive values and cause gradual discharge as described in the preceding section for the unbalanced cell. Fig. 10 illustrates this situation.

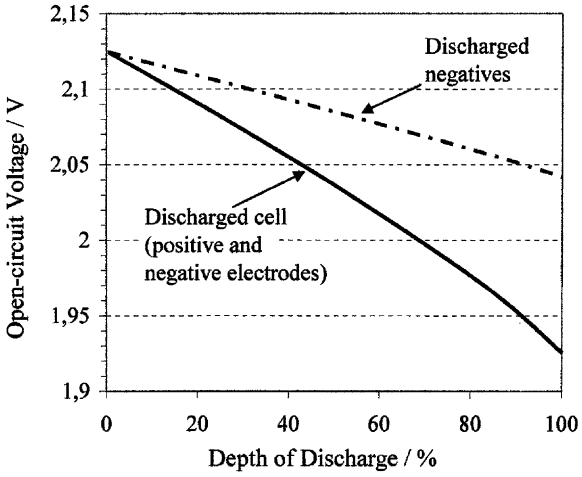

Fig. 9. Open-circuit voltage vs. depth of discharge (DOD), caused by acid dilution. The continuous line indicates the relation when both electrodes are discharged according to Eq. (1). The broken line represents the relation when only the negative electrode is discharged (Eq. (1b)).

The left part of Fig. 10 describes the same situation as shown in Fig. 8 for the overcharging voltage of 2.25 V per cell. Hydrogen evolution at the negative electrode exceeds grid corrosion in the positive electrode, and a corresponding current equivalent of surplus oxygen cannot be reduced, since this share of the overcharging current is already consumed by the excess of hydrogen evolution. As a consequence, the negative electrode is depolarized to a slightly positive polarization and "chemical discharge" occurs according to:

$$\text{Oxidation of the lead}: \quad 2Pb + O_2 \Rightarrow 2PbO \tag{7a}$$

Subsequent reaction with sulfuric acid :

$$2PbO + 2H_2SO_4 \Rightarrow 2PbSO_4 + 2H_2O \tag{7b}$$

In total self-discharge of the negative electrode :

$$2Pb + 2H_2SO_4 + O_2 \Rightarrow 2PbSO_4 + 2H_2O \tag{7}$$

which is another description of the anodic oxidation current in Section 4.2.

As long as the oxygen intake is limited so that it cannot shift the negative electrode to a positive polarization, the oxygen is reduced and acts as an additional anodic current that only reduces the polarization of the negative electrode. When, however, oxygen intake exceeds this limit, gradual discharge of the negative electrode occurs according to Eq. (7), as illustrated on the right hand in Fig. 10.

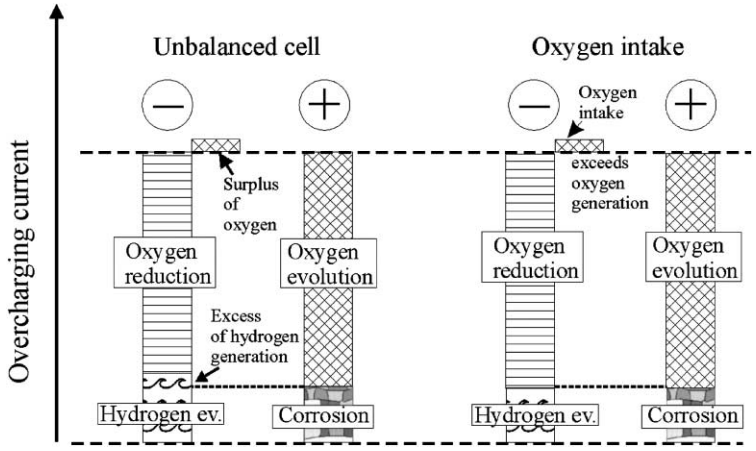

Fig. 10. Reasons that cause "discharged negatives". Left hand: imbalance by too high a rate of hydrogen evolution. Right hand: imbalance by oxygen intake.

For this reason, when "discharged negatives" are detected, it has to be checked whether there is actually an imbalance between hydrogen evolution and grid corrosion that causes the problem or whether the cell is not properly sealed. An indication would be that in the case of oxygen intake, normally only single cells within a battery will be affected.

4.2.2. Catalysts in VRLA batteries

The problem of discharged negative electrodes has been reported repeatedly in the USA, and this has mainly appeared with batteries designed for long service life (cf. e.g. [16]). The reason may be that, in such batteries, highly corrosion resistant alloys are combined with negative electrodes that evolve too much hydrogen. Jones presented a test for the negative active material and pointed out that material of the required purity should evolve at 25°C and open circuit (self-discharge rate) not more than 12 ml of hydrogen per day for each 100 Ah of capacity which means a current equivalent of about 1 mA/100 Ah [17]. This figure corresponds to the lower values for corrosion that have been mentioned in Section 4.1.2. (This balance depends, of course, also on the specific surface area of the positive grid.)

As mentioned in Section 4.1.1, such a high purity level may not always be available and a number of remedies, such as regularly repeated boost charges have been proposed and are in use. One other possibility is the installation of a small catalyst within the cell [18]. The effect of such a catalyst is illustrated in Fig. 11. Its principle is that the direct recombination of hydrogen and oxygen reduces the efficiency of the internal oxygen cycle, since a certain amount of the evolved oxygen does not reach the negative electrode. This "missing amount" of oxygen is directly recombined with

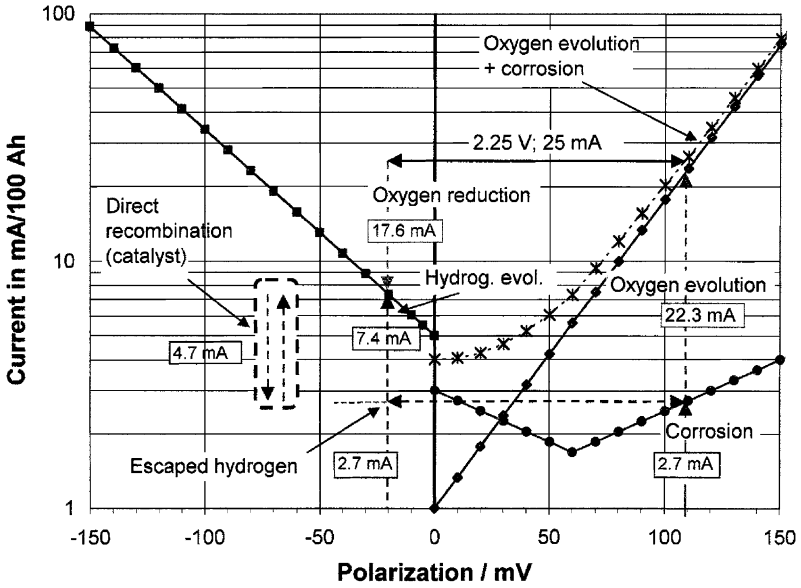

Fig. 11. Effect of a catalyst. Characteristic data as in Fig. 8. Efficiency of the catalyst is 4.7 mA or 21% of the internal oxygen cycle. The efficiency of the internal oxygen cycle is thereby reduced to 83%.

hydrogen by the catalyst and forms water vapor that is subsequently condensed to water within the cell. The electrochemical equivalent of this ''lost'' oxygen cannot be recombined at the negative electrode and a corresponding increased equivalent of hydrogen must be evolved to achieve the required current balance, and this means increased polarization of the negative electrode.

In Fig. 11, the basic situation corresponds to that in Fig. 8 at an overcharging voltage of 2.25 V. While in Fig. 8, this situation with 100% of recombination efficiency caused gradual discharge of the negative electrode equivalent to 1.9 mA/100 Ah, now the direct recombination of oxygen by the catalyst, equivalent to 4.7 mA, causes a deficit of oxygen, and requires a corresponding increase of hydrogen evolution. In Fig. 11, the negative electrode is polarized by −20 mV which in term reduces the polarization of the positive electrode correspondingly. Thus, the corrosion rate is also slightly reduced, and the amount of hydrogen that must escape from the cell equals this reduced corrosion rate.

Thus, the catalyst is effective in several respects.

- It stabilizes the potential of the negative electrode at a more negative polarization.
- Since the potential of the positive electrode is equally reduced, a corresponding reduction of the rate of corrosion and the float current is observed.
- Water loss is reduced to the rate of the (reduced) corrosion, since oxygen and hydrogen that directly are recombined remain as water in the cell.

Such catalysts have been in practical use since 1998 and experience so far supports the above statements [19].

Note: The situation of such a catalyst is absolutely different from those in ''recombination plugs'' that are known for vented lead-acid batteries (cf. e.g. [4], p. 259). Such recombination plugs are aimed to recombine as much as possible of the generated hydrogen and oxygen gases to reduce water loss. High recombination rates are required and thermal problems are the main concern, since the recombination generates much heat. The catalyst in the VRLA battery, on the other hand, has only to disturb the internal oxygen cycle and cause a small gap between oxygen evolution and the amount of oxygen that reaches the negative electrode. The efficiency of this catalyst can be very limited and this implies that no heat problems result.

5. Discharge performance

Discharge performance of VRLA batteries corresponds to that of the vented version, since the same reactions occur in both types. In general, discharge performance is degraded at lower temperatures, since the rates of the electrochemical reactions decrease while the resistance of the electrolyte is increased. At extremely low temperatures, freezing of the partly diluted acid in the discharged battery can increase its internal resistance dramatically, weaken the discharge performance and hinder recharging. At high temperatures, discharge performance is improved, but the life limiting factors grid corrosion and hydrogen evolution (together resulting in water loss) gain in importance.

The discharge performance of lead-acid batteries is principally handicapped for the following two reasons.

1. The participation of the acid in the cell reaction requires a sufficient amount of acid between the plates which again means a minimum spacing that must correspond to the thickness of the electrodes. Low internal resistance requires narrow spaced thin electrodes.
2. The unavoidable corrosion of the positive grid material requires a corresponding reserve of grid material when a long service life is desired.

The two requirements are in conflict and, as a consequence, long-lasting stationary or motive power batteries are based on thicker plates that are widely spaced, but these batteries are limited to a moderate load, while a high power output demand, e.g. with starter batteries in motor cars, is satisfied by thin and narrowly spaced plates which have a more limited service life.

The growing demand for high power output in modern uninterruptible power (UP) systems with short periods of power demand promoted the development of VRLA batteries, based on thin plates also for standby applications. The use of highly corrosion-resistant alloys and the necessity of minimum hydrogen evolution rates which are both required for minimum water loss, comply with this demand, and batteries, such as those shown in Figs. 1, 2 and 18, are nowadays in widespread use. A maximum service life of about 10 years is claimed for this type of battery under favorable conditions.

A design for extremely high loads in cycling applications has been realized in the ''Bolder thin metal battery'' [20,21], shown in Fig. 12. It is based on spirally wound foil electrodes that consist of thin foils (0.05 mm) of a lead tin alloy, coated on both sides by 0.075 mm layers of the active material. The AGM separator between the electrodes is only 0.18 mm thick. This battery has been developed for the use in tools, and is offered as a small cylindrical cell (2 V, 1.45 Ah) that can be loaded up to 800 W kg^{-1}, and 400 cycles to 100% depth of discharge (DOD) are claimed at the 2-h rate.

The bolder battery demonstrates the high discharge–charge capability that can be achieved with VRLA batteries. But the required foil-electrode technique is difficult to reconcile with unavoidable corrosion, and thus the calendar service life of this battery is limited.

Another approach to achieve extremely high loads up to 500 W kg^{-1} would be the use of thin bipolar plates [22]. The problem is, to find an electron conducting material that separates the two sides of the bipolar plate and is stable at the high potential of the positive electrode.

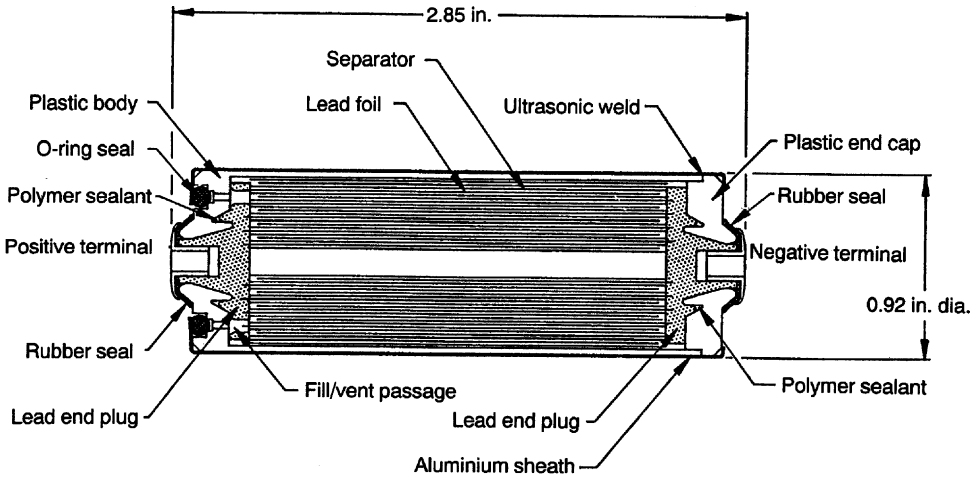

Fig. 12. Cross-sectional view of Bolder thin metal foil cell (TMF®). Cylindrical VRLA battery with foil electrodes: 2 V, 1.45 Ah at the 1.5 h rate (≈37 Wh kg^{-1}, ≈95 Wh dm^{-3}). Internal pressure: 1.38 bar = 1.38×10^5 Pa. Taken from [20].

6. Charge performance

Charging of valve-regulated batteries is also based on the same reactions as in the vented version. During charging, however, the secondary reactions gain in importance, and as mentioned in Section 4, at the end of the charging process the internal oxygen cycle characterizes the valve-regulated version, instead of water decomposition and a corresponding gas escape that occurs in vented batteries.

In stationary applications where the standby battery is continuously overcharged at a comparatively low float voltage, imbalance between hydrogen evolution and grid corrosion can cause the problems that have been described in Section 4.2. In applications where the battery is cycled, this problem is usually of minor importance, since a higher charging voltage must be applied to reach full charge within the, usually limited, charging period. The higher charging voltage increases the polarization of both electrodes and thus ensures sufficient recharge also of the negative electrode. Only in tight cycle applications with rather short charging periods, or after prolonged cycling operation, an imbalance between hydrogen evolution and grid corrosion can cause limiting negative electrodes due to insufficient recharge.

In Section 3.1, it has been shown as an advantage of VRLA batteries that overcharging is not required for mixing of the electrolyte. Nevertheless, in applications where the battery is cycled, a certain overcharge is usually applied even in the charging schedules of VRLA batteries for "equalizing". Such an overcharging compensates for variations of the internal oxygen cycle which consume a varying share of the overcharging current in the individual cells of a battery. Cells with a higher rate of the internal oxygen cycle (which acts as a parasitic current), may not reach full charge and may suffer a comparatively deeper discharge at the end of the subsequent discharge. During the following recharge, the situation will be aggravated. Thus, gradually the state of charge of the cells within a battery will become uneven, and premature failure of the "weak" cells may be the consequence. As a remedy, VRLA batteries usually are charged for a certain period at a constant voltage followed by a short period of "equalizing" at a slightly increased voltage or at a constant current that automatically increases the voltage.

Fig. 13 shows a typical charging schedule. At the beginning (Section I), the supply by the charger limits the charging rate, and a gradual increase of the cell voltage reflects the increasing open-circuit voltage due to increased acid concentration. During this charging period, the ohmic voltage drop remains nearly constant. The higher is the initial current, the steeper is the following decrease of the current, and the faster is full charge achieved. Besides this advantage, a high initial charging current proved to stabilize the positive active material and to increase the possible number of discharge–charge cycles [23] (a review with 125 references to original papers). When the specified voltage is reached (Section II), the current tapers down, and, if the charging period is long enough, finally reaches the rate of the float current given by the internal oxygen cycle. Section III is the equalization.

When fast charging is desired, the upper limit of the internal oxygen cycle has to be considered, especially during overcharging (equalizing) by a constant current. This

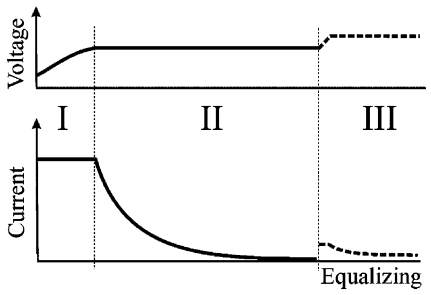

Fig. 13. Charging schedule typical for VRLA batteries "equalizing" may also mean a constant current or pulsed overcharging.

limit, the maximum rate of the internal oxygen cycle, is determined by the transport rate of oxygen. It depends mainly on the void volume that allows fast access of oxygen to the surface of the negative electrode, and, therefore, is increased with progressive water loss. In general, it is higher in AGM batteries than in gelled electrolyte batteries. Rough numbers of this maximum rate are 2 A/100 Ah in gelled electrolyte, while in a fairly dry AGM cell, it may even exceed 10 A/100 Ah. When the overcharging current exceeds this rate, a corresponding share of the generated oxygen can no longer reach the negative electrode and has to escape together with the corresponding equivalent of hydrogen. Actually, Häring and Giess [24] observed that a mixture of stoichiometric composition (33% of oxygen) escaped from the battery at extremely high rate recharges. This means that the VRLA battery partly operates as a vented one, and a correspondingly increased amount of water is lost during overcharging.

In connection with electric vehicle applications, a great number of tests have been performed and a number of charging schedules established. Pulsed currents are occasionally used for charging and "equalizing" (e.g. [21], p. 229), and to solve the problem of changing performance with age, various methods to terminate the charging process are proposed, e.g. constant voltage periods or pulses with open-circuit measurements during the pauses [25].

Furthermore, battery management systems (BMS) have been developed. In a "passive" version they monitor single-cell or group voltages, register the charged and discharged currents and establish the continual control of the state of the battery. In standby applications, such monitoring systems can largely reduce the number of capacity tests that otherwise are required to confirm the proper state of the battery. For cycling applications, especially in electric vehicles, but also in solar and wind energy applications, "active" battery management systems have been developed which balance the discharging–charging currents between the cells of a battery with the aid of parallel circuits. Overcharging as well as overdischarging of individual cells is thus avoided and the uniform state of the battery is preserved with the result of a more reliable performance and longer service life (a survey on BM systems will soon be published in [26]).

7. Heat effects

There are two sources of heat effects in batteries.

1. The reversible heat effect $T\Delta S$, determined by the thermodynamic data of the cell reaction.
2. Joule heating caused by kinetic parameters (overvoltage) and by the ohmic resistance of the conducting elements including the electrolyte (internal resistance).

The internal oxygen cycle represents a special form of Joule heating. This cycle consists of the two opposite reactions — oxygen evolution and oxygen reduction and thus the equilibrium voltage of the corresponding cell would be zero. Consequently, the cell voltage in total leads to polarization that causes heat generation.

The reversible heat effect is a thermodynamic parameter that describes the unavoidable heat absorption or heat emission connected with the cell reaction. It is strictly proportional to the amount of material that reacts and does not depend on discharge or charging rates. In the lead-acid battery, it is small, amounts to about 3.5% of the drawn or charged energy, and has the positive sign which means heat generation during charging and a corresponding cooling effect when the battery is discharged.

Joule heating is caused by current flow and is given by the product of polarization (=actual voltage minus open-circuit voltage) times current ($Q = (E - E_0) \times i$).

The heat that is generated in total is the sum of Joule heating and the reversible heat effect, and due to its sign, the latter reduces heat generation during discharge, but means additional heat generation during the charging process.

7.1. Heat effects during discharging

At very low discharge rates (discharge periods longer than 10 h), lead-acid batteries are slightly cooled by the reversible heat effect, but at increased discharge rates, the Joule heating exceeds the reversible heat effect and heat generation is observed. On the whole, heat generation during the discharge of lead-acid batteries is comparatively small. Calorimetric measurements, for example, showed that the discharge of small high rate batteries (Johnson Controls "Optima" 12 V, 16.5 Ah) generated <10% of the drawn energy as heat, even at a discharge rate of 5 C A [27]. The extent of heat generation depends of course on the internal resistance of the battery, but a high internal resistance limits high rate discharges, and in general, heat problems are not observed during the discharge of lead-acid batteries due to the limited amount of energy that is available (cf. e.g. Section 4.5.1 in [4]).

7.2. Heat effects during charging

The Situation is different during charging for three reasons.

1. The energy supply by the charging unit usually is not limited.
2. The rate of the secondary reactions is markedly increased with the increased voltage during charging which means a corresponding intensification of the internal oxygen cycle.
3. The reversible heat effect generates additional heat.

To illustrate the influence of the various heat generating effects, a schematic charging curve is shown in Fig. 14a. It is calculated corresponding to the characteristics plotted in Fig. 6, and a low internal resistance of 0.8 mΩ/100 Ah is assumed. Charging occurs at 2.4 V per cell, and initially the

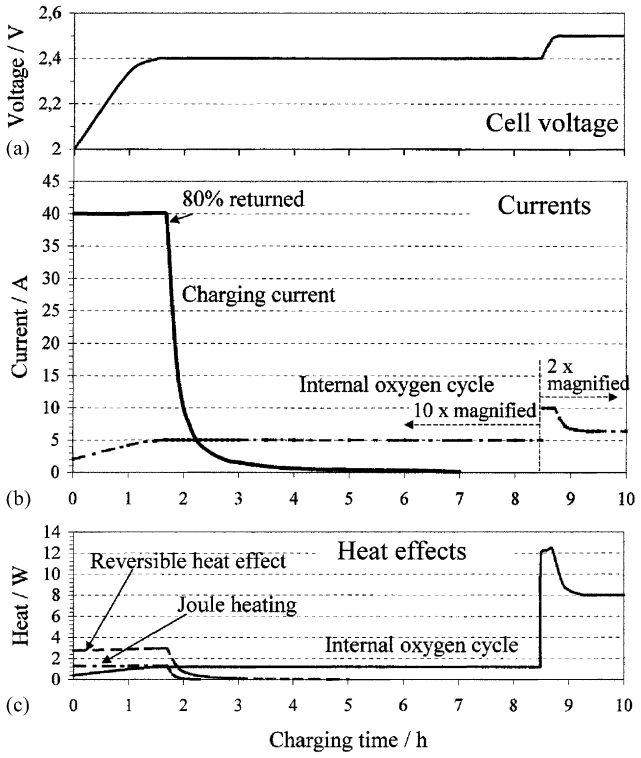

Fig. 14. Charging of a VRLA battery. Constant temperature and 100% of recombination efficiency assumed. Internal resistance: 0.8 mΩ (single cell). The 1.5 h "equalizing" at 2.5 V per cell at a current limit of 5 A. Heat generation in total: 31.2 Wh; reversible heat effect 5.7 Wh; Joule heating: 2.3 Wh; internal oxygen cycle: 23.2 Wh (13.5 Wh during equalizing).

current of 40 A/100 Ah ($4 \times I_{10}$) is limiting the charging rate (voltage drop: 32 mV). As an "equalizing step" overcharging for 1.5 h at 2.5 V at a maximum current of 5 A/100 Ah is assumed.

In Fig. 14b, the distribution of the current between charging and internal oxygen cycle is shown. The current share, consumed by the internal oxygen cycle is magnified by 10× during the initial phase and by 2× during equalizing. The sum of charging current and internal oxygen cycle would represent the charging current (hydrogen evolution and grid corrosion equivalents are not considered, since they are 2 orders of magnitude smaller than that of the internal oxygen cycle). In reality, the current would be slightly increased by heating the battery. This increase is not considered in Fig. 14.

Fig. 14c shows the heat generation by the various processes. At the beginning, the reversible heat effect dominates heat generation due to the high amount of material that is converted. Joule heating is proportional to the voltage drop, and caused by the current flow. The relation between the reversible heat effect and Joule heating is determined by the internal resistance of the battery. With batteries of higher internal resistance, Joule heating would dominate during this initial stage of the charging process (cf. e.g. Fig. 4.15 in [4]).

When the charging voltage is reached, the current decreases and this affects heat generation by the reversible

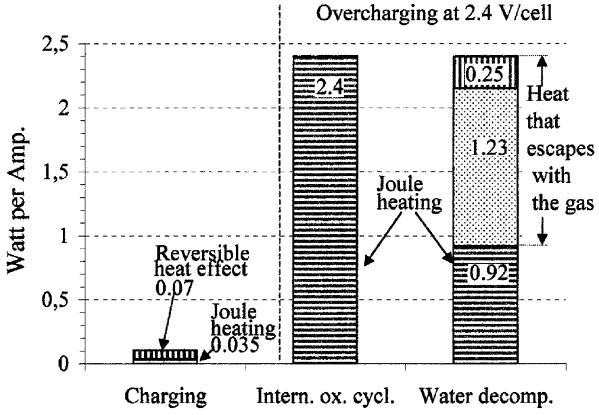

Fig. 15. Heat generation by the various reactions referred to a current of 1 A. For the internal oxygen cycle and water decomposition 2.4 V per cell of overcharging voltage are assumed. Joule heating depends on the internal resistance that for the comparison in Fig. 14 is assumed to 0.8 mΩ/100 Ah of nominal capacity.

heat effect and by Joule heating, while heat generation by the internal oxygen cycle remains constant, corresponding to the value of the constant cell voltage (which actually would slightly be increased by a rise in temperature).

Fig. 14 shows the strong heating effect caused by the internal oxygen cycle. The current share consumed by this reaction is very small and had to be magnified to be recognized in the current comparison. But the total heat generation is largely determined by the internal oxygen cycle, especially during the "equalizing step", which in Fig. 14 causes 13.5 Wh of heat, and so nearly half of the total heat generated. Actually, an even larger heat generation is to be expected, since, as already mentioned, the calculation did not consider how the heat increase within the cell during charging would increase the rate of the internal oxygen cycle.

The reason for the dominating heat effect of the internal oxygen cycle is illustrated in Fig. 15. Heat effects connected to the charging reaction are small, and their component caused by Joule heating depends on the internal resistance. The internal oxygen cycle, on the other hand, converts all the electrical energy into heat, since the reaction at the positive electrode is reversed at the negative, and thus the equilibrium voltage across the cell of this reaction would be zero.

For comparison, Fig. 15 also shows the situation of water decomposition with subsequent gas escape as it occurs in vented lead-acid batteries. In this case, most of the energy escapes as energy content of the gas from the cell. It consists of the following two components:

1. the product of the equilibrium voltage of 1.23 V (Eq. (2)) × current and
2. the reversible heat effect of water decomposition which amounts to about 20% of the converted energy and means additional energy consumption during electrolysis that increases the energy content of the escaping oxygen–hydrogen mixture. (20% of 1.23 V is 0.25 V, and the sum of both results in the calorific voltage of

1.48 V for water decomposition which is used in calorific calculations.)

In the vented battery, only the smaller share of the heat, generated by overcharging, remains within the cell while overcharging generates much more heat in VRLA batteries. For this reason, more attention has to be paid to heat generation in VRLA batteries compared to their vented counterparts.

7.3. Heating of the battery

Temperature increase or decrease of a battery during charging or discharging is described by

$$\frac{dT}{dt} = \frac{1}{C_{batt}}\left(\frac{dQ_{gen}}{dt} - \frac{dQ_{diss}}{dt}\right) \quad (J\,s^{-1}\ \text{or}\ W) \tag{8}$$

where dQ_{gen}/dt is the generated heat per unit of time and dQ_{diss}/dt is the dissipated heat per unit of time.

The heat capacity of the battery C_{batt} is given by

$$C_{batt} = \frac{\sum m(i)C_p(i)}{\sum m(i)} \quad (kJ\,kg^{-1}\,K^{-1}) \tag{9}$$

where $m(i)$ is the component i (kg) and $C_p(i)$ is the specific heat of component i ($J\,kg^{-1}\,K^{-1}$).

The specific heat C_p of VRLA batteries is in the range of 0.7–0.9 $kJ\,kg^{-1}\,K^{-1}$, while the corresponding value of vented lead-acid batteries is slightly above 1 $kJ\,kg^{-1}\,K^{-1}$. Differences are mainly caused by the varying content of electrolyte with its high specific heat capacity.

Eq. (8) points out that two parameters of equal weight determine heating of the battery.

- Heat generation within the battery.
- Heat dissipation from the battery.

Heat dissipation increases with a growing temperature difference between the battery and its surroundings, and a stable temperature of the battery is reached at a certain ΔT when heat generation balances heat dissipation, i.e. when $dQ_{gen}/dt = dQ_{diss}/dt$. If heat generation increases faster with temperature than heat dissipation, "thermal runaway" results. But normally this does not happen with VRLA batteries that regularly are controlled (cf. [4], p. 140).

Eq. (8) simultaneously indicates the importance of heat dissipation: if dQ_{diss}/dt in Eq. (8) is 0 (adiabatic situation where heat dissipation is not possible), it is only a question of time, until the battery will exceed any temperature limit, even at a very small heat generation.

Proper heat management of a battery is not only aimed to avoid too high a temperature, it is also intended to keep all cells of a battery within a range of temperatures that is as small as possible. Otherwise, the strong influence of the temperature on aging would cause different states of the individual cells (state of charge (SOC) as well as state of health (SOH)), depending on their location within the battery. Then charging and discharging performance of the individual cells would no longer be uniform, and premature failure of the cells that are in an unfavorable location will cause failure of the whole battery.

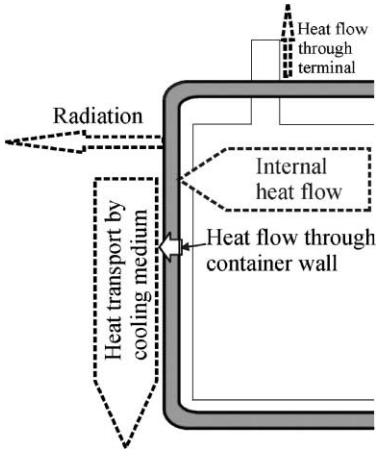

Fig. 16. The various ways of heat escape from the battery

7.4. Heat dissipation, cooling of the battery

Heat exchange of a battery with its surroundings proceeds in various ways. For the emission of heat these ways are sketched in Fig. 16. A corresponding figure with all the arrows reversed would apply for heat absorption from a warmer surroundings.

Three mechanisms are involved in this heat exchange.

1. Heat radiation.
2. Heat flow through a medium, e.g. the components of the battery and the container wall.
3. Heat transport by a medium.

Usually they occur in combination.

Fig. 16 indicates that cooling of batteries mostly occurs via their side walls. The bottom surface usually is in contact with a base which attains the same temperature as the battery, except if the battery is equipped with cooling channels in the bottom. The upper surface usually has little importance for heat exchange, since the lid has no direct contact with the electrolyte, and the intermediate layer of gas hinders heat exchange because of its low heat conductivity (Table 1). Moreover, in monobloc batteries, the cover often consists of more than one layer. Heat flow through the terminal normally can also be neglected, since the distance to the electrodes is rather long and often the terminals are covered by plastic caps. (Cooling through the terminal has occasionally been applied with submarine batteries which are equipped with massive copper terminals.)

7.4.1. Heat radiation

Heat radiation occurs according to the law of Stefan–Boltzmann:

$$\frac{dQ}{dt} = \varepsilon\sigma T^4 \quad (W\,m^{-2}) \tag{10}$$

Table 1
Heat conductance (λ, in Eq. (13)) of some materials at room temperature

Material	Heat conductance ($W\,m^{-1}\,K^{-1}$)
SAN	0.17
PVC	0.16
Polypropylene (PP)	0.22
Water	17
Lead	35
Iron	80
Copper	400
Hydrogen	10.5×10^{-5}
Air	1.5×10^{-5}

where ε is the Stefan–Boltzmann constant (5.67×10^{-8} $W\,m^{-2}\,K^{-4}$), σ the emission ratio of the material with respect to an ideal emitter (ca. 0.95 for usual plastic materials that are used for battery containers) and T is the absolute temperature (K).

The fourth power of T in Eq. (10) means a very strong dependence on temperature. Heat radiation always happens from the warmer to the colder part, and there is no heat flow between elements having the same temperature.

The heat-flow by radiation between two elements A, B is

$$\frac{dQ}{dt} = \varepsilon\sigma[T(A)^4 - T(B)^4] \quad (W\,m^{-2}) \tag{11}$$

This also applies when one of these elements is the surroundings.

For comparatively small temperature differences from environmental temperature, heat dissipation amounts to:

$$\frac{dQ}{dt} \approx 5{-}6\,W\,m^{-2}\,K^{-1} \tag{12}$$

which means that a battery emits by radiation about 5–6 $W\,m^{-2}$ of surface for each K (or °C) of difference between its container-surface and a lower environmental temperature. If the temperature of the surroundings is higher, a corresponding amount of heat will be absorbed.

7.4.2. Heat flow by conductivity

Heat flow through a medium is determined by its heat conductivity and by the distance that has to be passed. It is described by

$$\frac{dQ}{dt} = f\lambda\frac{\Delta T}{d} \quad (W) \tag{13}$$

where f is the surface area in m^2, λ the specific heat conductance ($J\,s^{-1}\,m^{-1}\,K^{-1}$) and d is the thickness of the medium (e.g. the container wall) (m).

The specific heat conductance of some materials that are of interest in connection with batteries or their surroundings are compiled in Table 1.

Table 1 shows that, for plastic materials, λ is in the order of 0.2 $W\,m^{-1}\,K^{-1}$. Thus, heat conduction through the container wall can be approximated

$$\frac{dQ}{dt} = \frac{200\,\Delta T}{d} \quad (W\,m^2\,K^{-1} \text{ for } d\,(mm) \text{ of wall thickness}) \tag{14}$$

The heat conductivity of water is about 100 times higher, and that of lead again is higher by another factor of 3. This means that the internal heat flow in Fig. 16 is fast compared to that through the container wall, mainly due to the heat conductivity of the electrodes, and the temperature measured at the sidewall usually represents a good approximation of the average cell temperature. This is no longer true at very high loads. Thus, with 155 Ah monoblocs, temperature differences up to 15 K have been observed between the center and the surface during high rate discharges (about 6 min of discharge duration) [24].

7.4.3. Heat transport by a medium

The most simple way of cooling by heat transport is free convection of air at the outer vertical surfaces which usually is applied to stationary batteries. It depends on the height of the cells or monoblocs and amounts for small differences ΔT to:

$$\frac{dQ}{dt} \approx 2{-}4\,W\,m^{-2}\,K^{-1} \tag{15}$$

These figures hold only for free air convection which requires a minimum distance of about 1 cm between facing walls (cf. [4], p. 39). Appropriate spacing of battery blocks should always be provided.

Comparison between Eqs. (13) and (15) indicates the importance of energy dissipation by radiation even at room temperature (which is often underestimated). Consequently, uniform radiation conditions should be observed, when a battery is installed. Heated surfaces in the neighborhood (e.g. from rectifiers) must be well shielded.

To give a rough indication of what the above figures mean, the monobloc battery shown in Fig. 17 will be used as an example. If this battery is standing free, as is usual in a stationary standby operation, heat dissipation from an inner cell would mainly occur via one sidewall, since the other sidewalls contact cells that have the same temperature and, therefore, do not allow heat emission. The surface area of the side wall would be $3.8\,cm \times 16.4\,cm = 62\,cm^2$ or $6.2 \times 10^{-3}\,m^2$.

According to Eqs. (12) and (15), radiation and free convection of air would allow heat emission of about 8 $W\,m^{-2}\,K^{-1}$, i.e. 0.05 W per cell sidewall and K. An assumed thickness of the container wall of 3 mm would allow the heat flow of 66 $W\,m^{-2}\,K^{-1}$ or 0.4 W per cell sidewall and K.

When the characteristics of Fig. 6 would apply to this battery, continuous overcharging at 2.3 V per cell would cause heat generation by the internal oxygen cycle of $2.3 \times 0.070 \times 100/26 = 0.62$ W/100 Ah, and the emission of the heat would result in

- $\Delta T = 1.5$ K across the container wall and
- $\Delta T = 12.4$ K at the surface of the battery.

Fig. 17. The 36 V starter battery, nominal capacity: 26 Ah (*C*/20) AGM technology. The battery contains two rows of 18 cells. The valve openings are to be seen in the lid. Size: H 8 (EN: L5); length: 339 mm; width: 174.8 mm; height: 164.5 mm; weight: 30 kg. By courtesy of VB batteries AG.

Altogether a temperature difference of 14 K against the surroundings would result. This rough calculation is made under the unfavorable assumption that only the small surface of the sidewall emits heat, but it indicates the limits of this ''natural cooling''.

Reduction of the overcharging voltage to 2.25 V per cell which is more normal for float charging would reduce the current to 30 mA, and thus heat generation by the internal oxygen cycle to 0.26 W/100 Ah, i.e. to about 40% and thus the temperature difference across the container wall would be reduced to 0.8 K and the total temperature difference to 7 K.

7.4.3.1. Forced cooling. Forced cooling systems have mainly been developed for electric vehicles, to prevent overheating and to attain uniform temperature in the inner and outer cells in larger batteries [28]. A simple method uses air that is blown by a fan through channels that are formed by the spacing of the cells or monoblocs within the battery. The low specific heat of air and its low specific heat conductance, however, limit this method. More effective cooling media are mineral oil and water. The first has the advantage that it cannot cause short circuits, but its specific heat content is rather low, at least compared to water which proves to be most effective. A widespread method uses pockets of plastic material that are arranged between the cells or blocks (along the sidewalls) and through which the cooling medium passes.

For comparison, some figures are compiled in Table 2.

Table 2
Heat dissipation by various mechanisms[a]

Heat dissipation process	Heat dissipation ($W\ m^{-2}\ K^{-1}$)	Sources
Radiation	5–6	Eq. (12)
Heat flow through a plastic wall of thickness *d* (mm)	200/*d*	Eq. (14)
Heat transport by vertical free air convection[b])	2–4	[4], p. 40
Forced air flow	25	–[c]
Forced flow of mineral oil	57	–[c]
Forced flow of water	390	–[c]

[a] Especially the figures for forced flow depend on a large number of parameters, e.g. design of the cooling system, flow rate, etc., and the values listed here can only be considered as a rough comparison gained by a particular experiment.

[b] Assumes sufficient spacing of the cells provided.

[c] Measured with an Optima battery for a uniform mass flow of the cooling media of 50 $g\ s^{-1}$ [28].

8. Future aspects

VRLA batteries have, within a short period of time, gained a strong position in the market, and have displaced their vented counterparts in many stationary applications. They offer a number benefits, such as largely reduced maintenance, extremely low hydrogen generation, no acid fumes, and room-saving installation by horizontal positioning. Thus, the strong position of lead-acid batteries in this field will be improved by the valve-regulated design, and they will remain in widespread use in the future. Furthermore, the VRLA design opens applications for lead-acid batteries where acid stratification had been an obstacle for the vented design.

At present, hybrid electric vehicles are being developed rapidly. Today most of them are equipped with nickel/metal hydride batteries since the battery is comparatively small and can be heavily loaded. If hybrid electric vehicles, however, are to be produced on a large scale, VRLA batteries will definitely be considered as an alternative, due to their comparatively low price. This applies especially to vehicles with larger batteries.

In conventional motor car development, fundamental changes are also on the way since the future electrical power net in the car will be based on a 36/42 V system [29]. Otherwise, the contradictionary demands of increased comfort and fuel saving could not be fulfilled. The architecture of the new network is not yet quite settled, and the choice of the batteries is still open. Some of the planned novelties, like the integrated starter generator (ISG), may demand loads so heavy that they may be beyond the capability of the lead-acid system. A long service life is indispensable for automobile batteries, and this might be a problem for VRLA batteries designed for extremely high loads, as has been mentioned in connection with Fig. 12. But for the next generation of car batteries, lead-acid batteries will be preferred, if they can fulfill the demands, because of their comparatively low price.

Two batteries that are developed for this application are shown in Figs. 17 and 18.

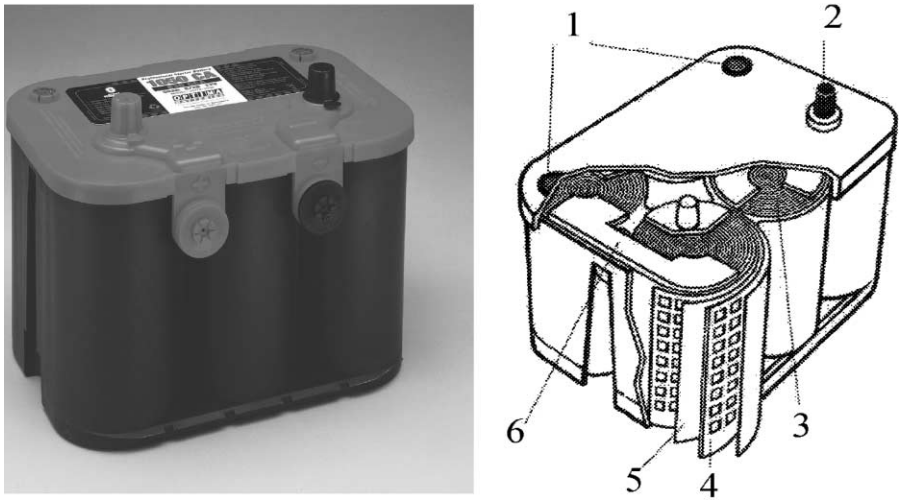

Fig. 18. VRLA battery Optima (12 V; 56 Ah (*C*/20)) with spirally wound electrodes. Length: 254 mm; width: 175 mm; height: 198 mm; weight: 17.5 kg; internal resistance: 30 mΩ. Construction details (right hand figure): (1) valves; (2) terminals; (3) spirally wound electrodes; (4) punched lead grid; (5) AGM separator; (6) cast-on straps and intercell connectors (by courtesy of Johnson controls).

The arrangement of the 18 cells in the monobloc of Fig. 17 in two rows equalizes the cooling surfaces for most of the cells, except the end cells.

Fig. 18 shows the Optima battery which represents a further development of the GATES battery, shown in Fig. 2. It is in wide use for various applications and three of these monoblocs could be combined to form a 36 V starter battery.

Thus, the development of lead-acid batteries goes on, and they will remain in widespread use, not always as the ''super star'' but mostly as the ''work horse''.

References

[1] H. Tuphorn, in: H.A. Kiehne (Ed.), Gerätebatterien, 3dr Edition, Expert Verlag, Ehningen bei Bŏblingen 2001, p. 36.
[2] GATES, Battery Application Handbook, GATES Energy Products (now HAWKER).
[3] Prospect data of EXIDE–GNB, by courtesy of EXIDE Europe.
[4] D. Berndt, Maintenance-Free Batteries, RSP Ltd. and Wiley, New York, 1997.
[5] A.L. Ferreira, The Battery Man, Vol. 41, No. 5, 1999, p. 70.
[6] Sandia National Labs and GNB, Batteries International, Issue 47, April 2001, p. 53.
[7] U. Teutsch, in: Proceedings of the 1st Telescon Meeting, Berlin, © IEEE Communications Society, 1994, p. 89.
[8] D. Berndt, R. Bräutigam, U. Teutsch, in: Proceedings of the 17th Intelec Meeting, The Hague, © IEEE Communications Society, 1995, p. 1.
[9] Implementation of the Mercury-Containing and Rechargeable Battery Management Act, published by the U.S. Environmental Protection Agency (EPA) as EPA530-K-97-009, http//www.epa.gov.
[10] D. Berndt, J. Power Sources 95 (2001) 2.
[11] T. Schnull, The Battery Man, Vol. 41, No. 10, October 1999, p. 66.
[12] B. Culpin, M.W. Pilling, F.A. Fleming, J. Power Sources 24 (1988) 127.
[13] R.D. Prengamam, J. Power Sources 95 (2001) 224.
[14] R.K. Jaworski, in: Proceedings of the 20th Intelec Meeting, San Francisco, USA, © IEEE Communications Society, 1998, p. 289.
[15] S. Piller, M. Perrin, A. Jossen, J. Power Sources 96 (2001) 113–120.
[16] W.E.M. Jones, D.O. Feder, in: Proceedings of the 18th Intelec Meeting, Boston, MA, 1996, p. 358.
[17] W.E.M. Jones, in: Proceedings of the 22nd Intelec Meeting, Phoenix, AZ, © IEEE Communications Society, 2000, p. 447.
[18] W.E.M. Jones, H.A. Vanasse, C.E. Sabotta, J.E. Clapper, E.F. Price, in: Proceedings of the 20th Intelec Meeting, San Francisco, USA, 1998, p. 461.
[19] S.S. Misra, T.M. Noveske, S.L. Mraz, A.J. Williamson, J. Power Sources 95 (2001) 162.
[20] Editorial note Batteries International, Issue 19, April 1994, p. 36.
[21] D.A.J. Rand, R. Woods, R.M. Dell, Batteries for Electric Vehicles, Research Studies Press Ltd., 1998, p. 218.
[22] M. Saakes, C. Kleijnen, D. Schmal, P. Have, J. Power Sources 95 (2001) 68.
[23] E. Meissner, J. Power Sources 78 (1999) 99–114.
[24] P. Häring, H. Giess, J. Power Sources 95 (2001) 153.
[25] M.A. Keyser, A. Pesaran, M.M. Mihalic, B. Nelson, in: Proceedings of the 17th Electric Vehicle Symposium, Montreal, October 2000, available at www.ctts.nrel.gov/BTM.
[26] A. Jossen, Valve-Regulated Lead-Acid Batteries, Elsevier, Amsterdam, to be published at the end of 2001.
[27] A.A. Pesaran, M. Keyser, Annual Battery Conference, Long Beach, January 2001, available at www.ctts.nrel.gov/BTM.
[28] A.A. Pesaran, Advanced Automotive Battery Conference, Las Vegas, NE, February 2001, available at www.ctts.nrel.gov/BTM, reprinted in Batteries International, Issue 47, April 2001, p. 107.
[29] H.-M. Graf, The Battery Man, Vol. 43, May 2001, p. 64.